Raman scattering from microcrystals of MgO

H. K. Böckelmann*
Department of Physics, King's College, Strand, London WC2R 2LS, United Kingdom

R. G. Schlecht
Department of Physics, Southern Illinois University, Carbondale, Illinois 62901

(Received 20 June 1974)

Raman scattering has been observed from microcrystals of MgO which were produced from $Mg(OH)_2$, $MgCO_3$, and MgO smoke. Particles which had an average diameter of 300 Å gave Raman bands with frequency shifts of 595, 719, and 1096 cm^{-1}, whereas particles of mean diameter 600 Å gave bands at 592 and 1088 cm^{-1}. These results are discussed in terms of the macroscopic and microscopic theories that have been used to describe the lattice dynamics of small crystals. Experimental evidence of the inverted Lyddane-Sachs-Teller relation is given.

I. INTRODUCTION

The vibrational properties of finite diatomic ionic crystals have received considerable attention recently. Theoretical studies have been performed on different geometries from the microscopic (slab,[1-6] sphere[7,8]) and macroscopic (slab,[9-13] cylinder,[9,10,14] and sphere[9,10,15-18]) points of view. Various experimental studies have been made on the vibration of finite crystals of MgO using infrared absorption,[19,20] neutron scattering,[21] and electron scattering[22,23] techniques.

In this paper we report the experimental study of oscillations of microcrystals of MgO using laser Raman spectroscopy. A large MgO crystal shows no first-order Raman spectrum, but the microcrystals showed three lines, 595, 719, and 1096 cm^{-1}, which were independent of the compound from which the MgO microcrystals had been produced, but which varied in frequency and relative intensity with the size of the MgO particles. These results are compared with those obtained by other experimental methods, and with the predictions of the various theoretical studies. Experimental evidence of the so-called inverted Lyddane-Sachs-Teller relation is given by these results.

II. THEORY

A. Macroscopic theory

The macroscopic theory uses Maxwell's equations and the appropriate boundary conditions. The first theoretical study on a diatomic ionic sphere was done by Fröhlich.[15] If ϵ_0 and ϵ_∞ represent the static and high-frequency dielectric constants of the specimen and if ω_{TO} and ω_{LO} are the transverse-optical and longitudinal-optical frequencies of the corresponding infinite crystal, respectively, Fröhlich obtained (Fröhlich mode),

$$\omega_S^2 = [(\epsilon_0 + 2)/(\epsilon_\infty + 2)]\,\omega_{TO}^2 . \tag{1}$$

Using the Lyddane-Sachs-Teller relation

$$\omega_{LO}/\omega_{TO} = (\epsilon_0/\epsilon_\infty)^{1/2}, \tag{2}$$

ω_S^2 takes the form

$$\omega_S^2 = (\epsilon_\infty/\epsilon_0)[(\epsilon_0 + 2)/(\epsilon_\infty + 2)]\omega_{LO}^2 . \tag{3}$$

From Eqs. (1) and (3) we observe that there exists only one single mode, the so-called Fröhlich mode, and, since $\epsilon_\infty < \epsilon_0$ for an ionic crystal, ω_S^2 falls in the transverse-optical–longitudinal-optical gap (TOLOG).

Ruppin and Englman[9,10] analyzed a diatomic sphere immersed in a medium of dielectric constant ϵ_M, with and without retardation. If the displacement of the ions is (a) divergence free, the equations of motion have as solutions the transverse-optical mode ω_{TO} of the infinite crystal; (b) curl free, the solutions give the customary longitudinal-optical frequency ω_{LO}; (c) divergence and curl free, the so-called surface modes are obtained. Taking the electronic polarizability and condition (c) and neglecting retardation they found a series of modes in the TOLOG [Ruppin-Englman mode (REM)],

$$\omega_L^2 = \{[L\epsilon_0 + \epsilon_M(L+1)]/[L\epsilon_\infty + \epsilon_M(L+1)]\}\,\omega_{TO}^2, \tag{4}$$

where $L = 1, 2, 3\ldots$. If retardation is included they obtained (REMR)

$$\omega_L^2 = \frac{L\epsilon_0 + \epsilon_M(L+1)(1+\Gamma)}{L\epsilon_\infty + \epsilon_M(L+1)(1+\Gamma)}\,\omega_{TO}^2, \tag{5}$$

where $L = 1, 2, 3\ldots$;

$$\Gamma = \tfrac{6}{5}\epsilon_M[(\epsilon_0 + 2\epsilon_M)/(\epsilon_\infty + 2\epsilon_M)](\omega_{TO}R/C)^2 ,$$

where R is the radius of the sphere and C is the velocity of light. For small values of R, $\Gamma \ll 1$, then the result of Eq. (4) is regained. Besides the series in the TOLOG, there exist (i) a series of frequencies $\omega < \omega_{TO}$, which converges to ω_{TO} as the particle size approaches zero, and (ii) a series

of modes with $\omega > \omega_{LO}$, which diverges to infinity as R goes to zero. A similar result was obtained by Fuchs and Kliewer[17] for very small particles using Mie's theory of scattering.

B. Microscopic theory

1. Phonons without retardation

The microscopic theory uses lattice dynamics to analyze the lattice waves of a finite crystal. Maradudin and Weiss[7] analyzed the limiting optical frequencies in alkali-halide crystals, neglecting retardation. Starting from the Kellerman[24] model they evaluated the elements of the dynamical matrix for a finite crystal of spherical shape of radius R. The 6×6 determinant was solved for waves propagating in the [100], [110], and [111] directions. The six solutions for each case are (a) acoustic modes (three solutions)

$$\omega^2 = 0;$$

(b) transverse-optical modes [two solutions, Maradudin-Weiss, transverse (MWT)],

$$\omega_T^2 = (e^2/V_a)\mu(A + 2B - \tfrac{4}{3}\pi\Delta); \tag{6}$$

(c) longitudinal-optical mode (MWL),

$$\omega_L^2 = (e^2/V_a)\mu(A + 2B + \tfrac{8}{3}\pi\Delta), \tag{7}$$

where

$$\Delta = 1 - 3J_1(2\pi KR)/2\pi KR .$$

$J_1(2\pi KR)$ is the spherical Bessel function of first order; $\mu = (1/m_+ + 1/m_-)$; m_+ and m_- are the masses of the positive and negative ions, respectively; e is the effective electronic charge; r is the distance between nearest neighbors; $V_a = 2r_0^3$ is the volume of the unit cell.

The constants A and B are proportional to the first and second derivatives of the repulsive interaction potential between the ions. Further, A and B are related to the compressibility β by[24]

$$\beta = (1/6r_0)(e^2/V_a)(A + 2B). \tag{8}$$

The dependence of the frequencies on the size of the crystal is embodied in Eqs. (6) and (7) by the argument $(2\pi KR)$ of the spherical Bessel function. If the limit $R \to \infty$ is taken and then $K \to 0$ the results of Kellermann[24] for an infinite crystal are regained. Now, leaving R fixed and taking $K \to 0$, the transverse-optical and longitudinal-optical modes approach a common value[7]

$$\omega_0^2 = (e^2/V_a)(A + 2B). \tag{9}$$

The ratio of the longitudinal- and transverse-optical frequency is unity, therefore contradicting the Lyddane-Sachs-Teller relation, Eq. (2), at the $K \to 0$ limit.

2. Phonons with retardation

The previous analysis by Maradudin and Weiss has been extended by Lucas[8] to include retardation. Starting with a phonon-photon coupled Hamiltonian and using the formalism developed by Hopfield[25] in connection with the exciton theory, Lucas[8] found the following modes of vibration: (a) acoustical (three solutions),

$$\omega = 0;$$

(b) transverse optical (two solutions),

$$(\Omega_\pm)_T^2 = (e^2/2V_a)\mu[A + 2B + 4\pi(1 - \tfrac{1}{3}\Delta)] + \tfrac{1}{2}K^2C^2 \pm \tfrac{1}{2}\{[(e^2/V_a)\mu[A + 2B + 4\pi(1 - \tfrac{1}{3}\Delta)] - K^2C^2]^2 + (16\pi e^2K^2C^2/V_a)\mu\}^{1/2}; \tag{11}$$

(c) longitudinal optical,

$$\Omega_L^2 = (e^2/V_a)\mu(A + 2B + \tfrac{8}{3}\pi\Delta). \tag{12}$$

A, B, μ, and Δ have the same meanings as already defined.

The degeneracy of the three optical modes is lifted, as can be seen comparing Eqs. (11)–(13). Further, comparing Eqs. (5) and (11) we see that the longitudinal-optical mode is not affected by the retardation effects.

As can be observed from Eqs. (11) and (12) for small values of K, the Lyddane-Sachs-Teller relation, Eq. (2), is inverted,[8] or

$$\lim_{K\to 0}[\Omega_L^2/(\Omega_+)_T^2] = \epsilon_\infty/\epsilon_0 . \tag{13}$$

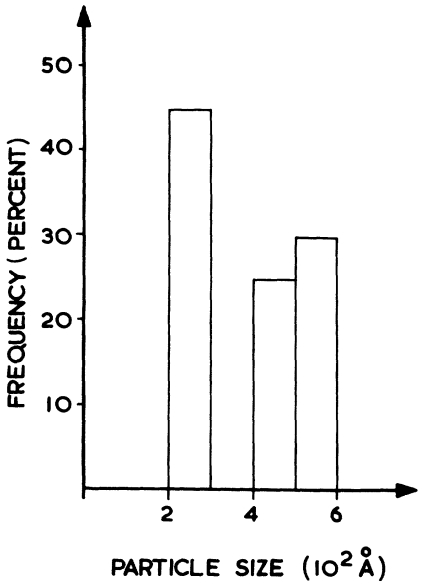

FIG. 1. Particle size distribution of MgO microcrystals produced by thermal decomposition of $Mg(OH)_2$ at 600 °C during 6 h.

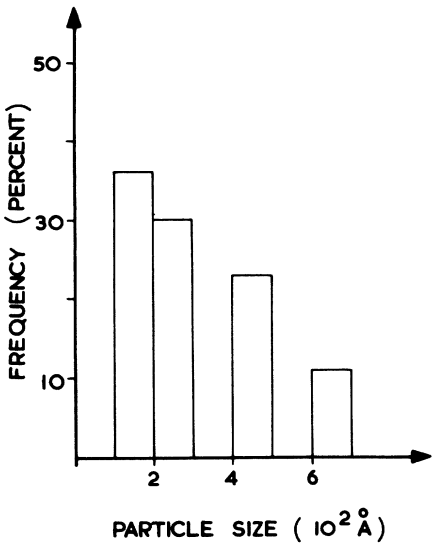

FIG. 2. Particle size distribution of MgO microcrystals produced by thermal decomposition of $MgCO_3$ at 600 °C during 6 h.

III. EXPERIMENT

A. Sample preparation and particle-size analysis

Magnesium oxide is a suitable compound for the study of finite crystal effects because (i) MgO is a cubic crystal; it possesses inversion symmetry, and therefore in the bulk has no first-order Raman spectrum; (ii) a large (330 cm^{-1}) transverse-optical–longitudinal-optical gap exists at the Brillouin-zone center of a large crystal; (iii) it is an ionic crystal of excellent physical stability that can be produced in powders of microcrystals of high purity and uniform size, ranging from 100 to over 1000 Å; (iv) the physical constants of MgO are well known; (v) it has a high melting point and it can therefore be freely exposed to the intense laser beam required by the Raman experiment.

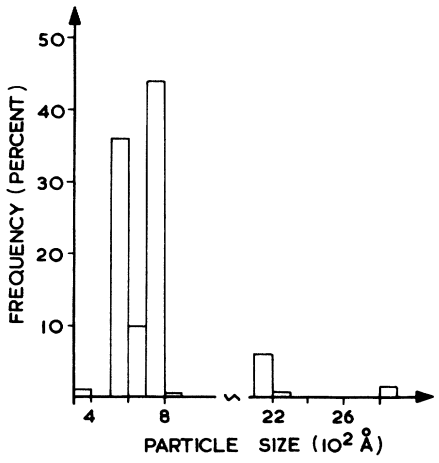

FIG. 3. Particle size distribution of MgO microcrystals produced by burning Mg ribbons in air.

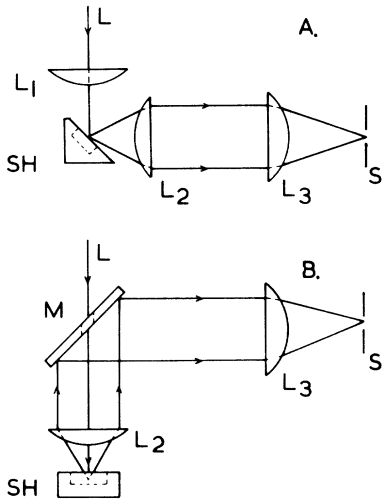

FIG. 4. Optical arrangement: (a) 90° scattering geometry; (b) back-scattering geometry.

Microcrystals of MgO were produced by three different methods: (a) thermal decomposition of $MgCO_3$ (Refs. 22, 26, and 27); (b) thermal decomposition of $Mg(OH)_2$; (c) burning Mg ribbons in air or oxygen. The thermal decompositions of $MgCO_3$ and $Mg(OH)_2$ were performed in a controllable platinum furnace using quartz or alsimag combustion boats. MgO smoke obtained from burned Mg ribbons in air was collected on glass plates. The single-crystal nature of the finite crystals was established by electron diffraction. The purity of the microcrystals was determined to be better than one part in 10 000 by x-ray diffraction.

The sizes of the microcrystals were controlled by calcination temperature and time. The particle-size analysis has been performed by x-ray line broadening using the Debye-Scherer theory[26,28] and

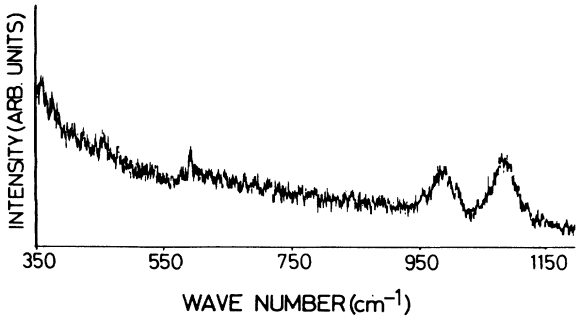

FIG. 5. Chart recording of the Raman spectrum of MgO microcrystals obtained by thermal decomposition of $Mg(OH)_2$ at 600 °C for 9 h. (Slits: 150 μm, scan: 20 cm^{-1}/min, Int. const.: 5 sec.)

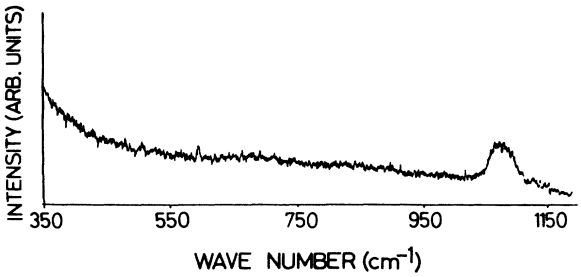

FIG. 6. Chart recording of the Raman spectrum of MgO microcrystal obtained by thermal decomposition of $MgCO_3$ at 600 °C for 6 h. (Slits: 150μm, Scan: 20 cm^{-1}/min, Int. const.: 5 sec.)

transmission electron microscopy. Figures 1–3 display the particle-size distribution obtained from electron microscopy. The histograms were obtained by measuring 200 particles in two dimensions. Close agreement has been obtained between the two methods for the average particle sizes. The MgO particles were pressed into small disks of $\frac{1}{2}$-in. diameter under a pressure of 800 lb/in.^{2}

B. Optics and detection

The optical systems which were used are shown in Fig. 4, where (A) and (B) show the 90° and back-scattering geometry, respectively. The laser beam (L) at 4880 Å, after traversing a narrow-band interference filter, was focused on the sample by a convex lens (L_1) of focal length 21 mm in the 90° scattering geometry. The scattered beam was collected by a wide angle (68°) short focal length (32 mm) lens (L_2). The lens L_3 focuses the collimated beam on the slit (S) to cover the first collimating mirror of the double monochronomator. In the back-scattering geometry the laser beam (L) was focused on the sample by the collecting lens (L_2). The collimated scattered beam after

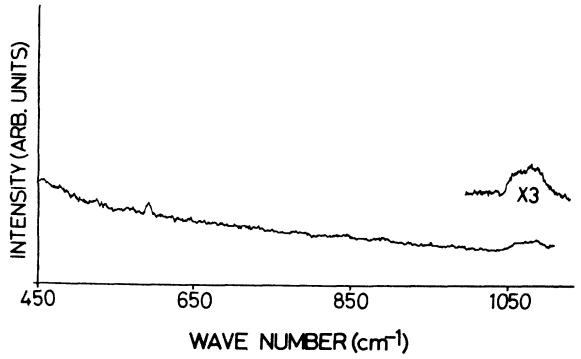

FIG. 7. Chart recording of the Raman spectrum of microcrystals of MgO obtained by thermal decomposition of $MgCO_3$ at 900 °C for 19.5 h. (Slits: 200μm, Scan: 20 cm^{-1}/min, Int. const.: 10 sec, Average particle size: 600 Å.)

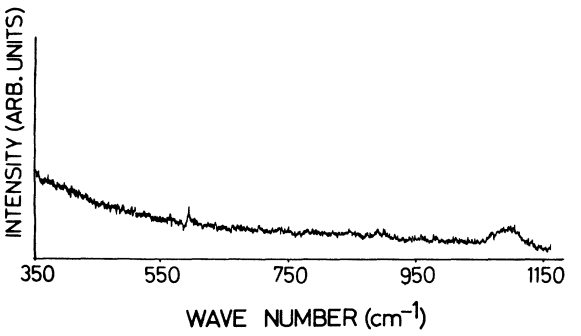

FIG. 8. Chart recording of the Raman spectrum of microcrystals of MgO obtained by burning Mg ribbons in air. (Slits: 150μm, Scan: 20 cm^{-1}/min, Int. const.: 10 sec.)

being deflected by the mirror (M) is focussed by the lens L_3 on the slit (S).

The dispersed beam was focused on a cooled Centronic 4249 10-mm-diam high-gain photomultiplier cathode. The electrical pulses were processed by the customary photon-counting method.

IV. RESULTS AND DISCUSSION

Figures 5–9 show the chart recordings of the Raman spectra (Stokes component) of microcrystals of MgO obtained from several different parent compounds.

The physical properties of MgO are listed in Table I. These physical properties have been used to predict the vibrational properties of spherical microcrystals of MgO, following the various available theoretical treatments. The predicted fre-

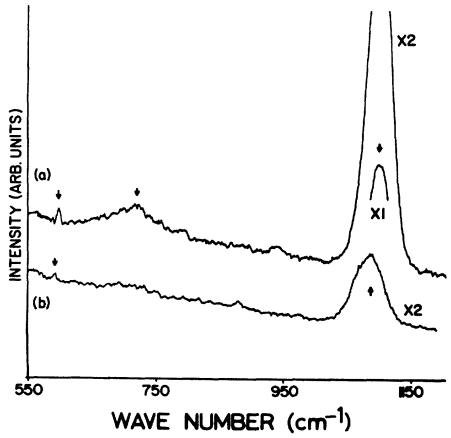

FIG. 9. Comparison of two different average particle sizes. MgO finite crystals obtained from thermal decomposition of $MgCO_3$. (a) Average particle size of 300 Å. (b) Average particle size of 600 Å. (Slits: 200μm, Scan: 10 cm^{-1}/min, Int. const.: 25 sec, Ref. 29.)

TABLE I. Physical properties of MgO.

Physical property	Value	Reference
Lattice constant r_0	2.1 Å	30
Compressibility β	5.95×10^{-13} cm^2/dyn	30
Static dielectric constant ϵ_0	9.64 (300 °K)	31
High-frequency dielectric constant ϵ_∞	3.01 (300 °K)	31
ω_{TO} (300 °K)	401 cm^{-1}	31
ω_{LO} (300 °K)	725 cm^{-1}	31
Effective charge e	0.88	32

quencies for particles having $R \ll C/\omega_{TO}$ are presented in Table II together with the frequencies observed in the Raman spectrum of MgO microcrystals. Note that none of the observed microcrystal frequencies has been observed in the two-phonon Raman spectrum of bulk MgO.[33]

As can be observed from the spectra the scattering intensity is particle size dependent; further, a small shift is observed when the average particle size varies from 300 to 600 Å. The line at 719 cm^{-1} observed for particles of 300 Å cannot be observed when the average particle size increases much above 300 Å. The Raman line at 978 cm^{-1} in Fig. 5 does not belong to the fundamentals of $Mg(OH)_2$,[34] neither can it be explained by the present theories. A shift of approximately 5 cm^{-1} towards higher frequencies has been observed by cooling the samples to 110 °K.

As can be seen from Table II, the macroscopic theories can explain the lowest mode observed in the TOLOG, but they fail to predict the higher-frequency modes. In Table II we have included the theoretical frequencies for MgO for $L=1$ and $L=\infty$. As L increases the mode becomes more localized near the surface of the particle, and therefore its scattering intensity decreases.[9] But as L becomes large the mode density becomes large at the limiting frequency ω_∞. However, for small crystallites the macroscopic theory predicts that the major part of the scattering is from the $L=1$ mode. As Table II shows, close agreement has been obtained in this experiment with the microscopic theory developed by Lucas.[8] The theory predicts that at $K=0$ the frequencies of the modes should all be size independent, whereas a small shift has been observed by varying the average particle sizes. However, as will be discussed later for small crystals K conservation is not required and the frequency shift may be due to the bending of the dispersion curve near $K=0$.

Figures 10–12 show the computer-generated dispersion curves using the theory of Lucas and the necessary constants given in Table I for 300-, 600-, and 10 000-Å particle sizes, respectively.

TABLE II. Summary of the theoretical and experimental values of finite crystal modes of vibration.

	Macroscopic theory		
Mode	Below TOLOG	TOLOG	Above TOLOG
Fröhlich	None	$\omega_s = 609$ cm^{-1}	None
REM and REMR	ω_{TO}	$\omega_1 = 609$ cm^{-1}	Infinite
		$\omega_\infty = 653$ cm^{-1}	
	Microscopic theory at $K=0$		
Mode	Below TOLOG	TOLOG	Above TOLOG
MWT + MWL	None	$\omega_L = \omega_T = 609$ cm^{-1}	None
Lucas	None	$\Omega_L = 609$ cm^{-1}	$\Omega_+ = 1100$ cm^{-1}
	Experimentally observed Raman lines (Stokes component, 300 °K)		
Average particle size (Å)	Below TOLOG	TOLOG	Above TOLOG
300	None	595 cm^{-1}	1096 cm^{-1}
		719 cm^{-1}	
600	None	592 cm^{-1}	1088 cm^{-1}
950	None	592 cm^{-1}	1088 cm^{-1}

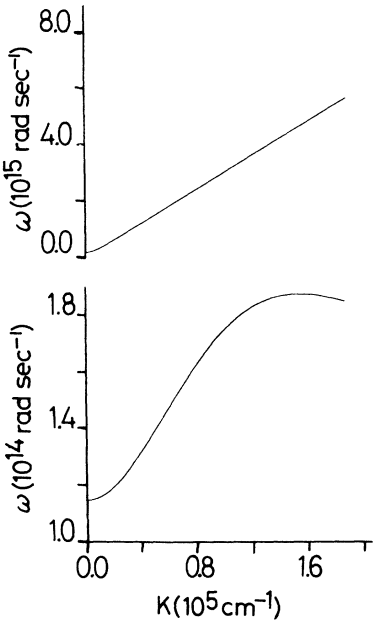

FIG. 10. Computer-generated dispersion curves using Eqs. (11) and (13) for 300-Å particle size.

Only the two optic modes are shown. The limiting value of the longitudinal-optical mode (for which the Kellermann model gives too high a value) is quickly approached for particles of 10 000 Å in the Lucas theory, Fig. 12, which is contrary to the prediction of the macroscopic theory.[10] Therefore, for particles of this size no first-order Raman spectrum should be observed.

The square of the ratio of the transverse-optical to the longitudinal-optical mode of the experimentally observed modes is 0.543, in close agreement with the theoretical value of 0.549 given by Eq. (13).

Since the uncertainty in the wave vector is of the order of $(1/2R)$, as given in Ref. 7, the conservation of momentum does not have to be considered for the particle sizes used in the experimental work.

Several other experimental techniques have been used to study the vibrations of microcrystals of MgO. The observed vibrations of MgO powders using infrared techniques vary considerably depending upon the starting parent compounds and the surrounding medium.[19,20,35,36] Modes have been reported below as well as inside the transverse-optical–longitudinal-optical gap, but none above. Many of the results are in disagreement with the macroscopic theory as well as the microscopic theory. In an attempt to obtain an agreement between theory and the observed modes, the concept of an average dielectric function has been introduced,[35,29] that is, including the effect of the neighboring particles and the surrounding medium on the dielectric function of the macroscopic theory, with only limited success.

The experimentally determined modes of vibration of MgO microcrystals by neutron scattering[21] are 172, 332, 504, and 610 cm^{-1}. Only the highest frequency can be considered to be in agreement

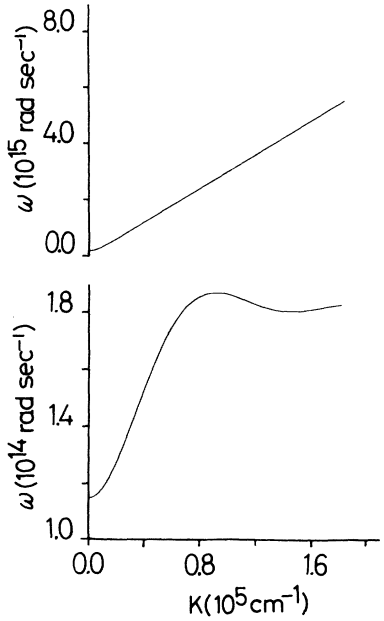

FIG. 11. Computer-generated dispersion curves using Eqs. (11) and (13) for 600-Å particle size.

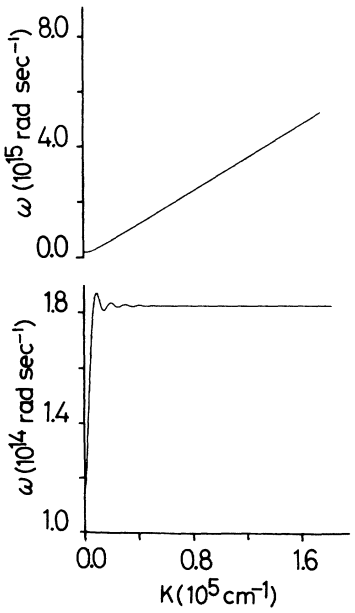

FIG. 12. Computer-generated dispersion curves using Eqs. (11) and (13) for 10 000-Å particle size.

with the experimental value found in this work. With electron scattering only the longitudinal mode can be detected.[21] Boersch *et al.*[22,23] deposited MgO smoke on collodion and found a broad line at 589 cm^{-1}. This value is in very close agreement with our observed value for the longitudinal-optical mode. In none of these experiments has a mode above TOLOG been found.

We have shown that laser Raman spectroscopy can be a useful tool in the study of finite crystals. Further experimental studies are necessary to elucidate the effect of surrounding medium other than air and vacuum.

ACKNOWLEDGMENTS

We would like to thank D. F. Clampet, C. W. Kinslow, L. A. Cristaudo, and H. Bank for their technical assistance during the course of this work. We would like to thank Dr. W. F. Sherman of King's College and Dr. B. L. Beers and Dr. M. E. Foglio of Southern Illinois University for helpful comments.

*Work performed in the Dept. of Physics of Southern Illinois University at Carbondale, Carbondale, Ill.

[1]S. Y. Tong and A. A. Maradudin, Phys. Rev. 181, 1318 (1969).
[2]A. Grimm, A. A. Maradudin, and S. Y. Tong, J. Phys. (Paris) Suppl. 31, C1-9 (1970).
[3]A. A. Lucas, J. Chem. Phys. 48, 3156 (1968).
[4]R. E. Allen, G. P. Alldredge, and F. W. de Wette, Phys. Rev. Lett. 23, 1285 (1969).
[5]T. S. Chen, G. P. Alldredge, and F. W. de Wette, Phys. Rev. B 6, 627 (1972).
[6]R. E. Allen, G. P. Alldredge, and F. W. de Wette, Phys. Rev. B 4, 1648 (1972).
[7]A. A. Maradudin and G. H. Weiss, Phys. Rev. 123, 1968 (1961).
[8]A. A. Lucas, Phys. Rev. 162, 801 (1967).
[9]R. Englman and R. Ruppin, J. Phys. C 1, 614 (1968).
[10]R. Ruppin and R. Englman, Rep. Prog. Phys. 33, 149 (1970).
[11]K. L. Kliewer and R. Fuchs, Phys. Rev. 144, 573 (1966).
[12]K. L. Kliewer and R. Fuchs, Phys. Rev. 150, 573 (1966).
[13]R. Fuchs, K. L. Kliewer, and W. J. Pardee, Phys. Rev. 150, 589 (1966).
[14]R. Englman and R. Ruppin, J. Phys. C 1, 1515 (1968).
[15]H. Fröhlich, *Theory of Dielectrics*, 2nd ed. (Oxford U. P., New York, 1950).
[16]R. Ruppin and R. Englman, J. Phys. C 1, 630 (1968).
[17]R. Fuchs and K. L. Kliewer, J. Opt. Soc. Am. 58, 319 (1968).
[18]T. H. K. Barron, Phys. Rev. 123, 1995 (1961).
[19]N. T. McDevitt and W. L. Baun, Spectrochim. Acta 70, 799 (1964).
[20]F. Brehat, O. Evrard, A. Hadni and J. P. Cambert, C. R. Acad. Sci. B 263, 1112 (1966).
[21]K. H. Rider and E. M. Hörl, Phys. Rev. Lett. 20, 209 (1968).
[22]H. Boersch, J. Geiger, and W. Stickel, Phys. Rev. Lett 17, 379 (1966).
[23]H. Boersch, J. Geiger, and W. Stickel, Z. Phys. 212, 130 (1968).
[24]E. W. Kellermann, Philos. Trans. R. Soc. Lond. 238, 513 (1940).
[25]J. J. Hopfield, Phys. Rev. 112, 1555 (1958).
[26]L. S. Bricks and H. Friedman, J. Appl. Phys. 17, 687 (1946).
[27]W. E. Kuhn, in *Ultrafine Particles*, edited by W. E. Kuhn (Wiley, New York, 1963), p. 41.
[28]*International Handbook of X-Ray Crystallography* (Kynock, Birmingham, 1952).
[29]R. G. Schlecht and H. K. Böckelmann, Phys. Rev. Lett. 31, 930 (1973).
[30]L. Genzel and T. P. Martin, Phys. Status Solidi B 51, 101 (1972).
[31]J. R. Jasperse, A. Kahan, J. N. Plendl, and S. S. Mitra, Phys. Rev. 146, 526 (1965).
[32]E. Burstein, in *Lattice Dynamics*, edited by R. G. Wallis (Pergamon, Oxford, 1965), p. 315.
[33]N. B. Manson, W. van der Ohe, and S. L. Chodos, Phys. Rev. B 3, 1968 (1971).
[34]G. R. Wilkinson, in *The Raman Effect*, edited by A. Anderson (Dekker, New York, 1973), Vol. 2.
[35]L. Genzel and T. P. Martin, Phys. Status Solidi B 51, 91 (1972).
[36]J. T. Luxon, D. J. Montgomery and R. Summit, Phys. Rev. 188, 1345 (1969).